symmetry

MDPI

Article

Fronto—Parietal Regions Predict Transient Emotional States in Emotion Modulated Response Inhibition via Low Frequency and Beta Oscillations

Siddharth Nayak [1] and Arthur C. Tsai [2,*]

[1] Department of Radiology, Weill Cornell Medicine, New York, NY 10021, USA; sin4005@med.cornell.edu
[2] Institute of Statistical Science, Academia Sinica, Taipei 11529, Taiwan
* Correspondence: arthur@stat.sinica.edu.tw

Abstract: The current study evaluated the impact of task-relevant emotion on inhibitory control while focusing on midline cortical regions rather than brain asymmetry. Single-trial time-frequency analysis of electroencephalography recordings linked with response execution and response inhibition was done while thirty-four participants performed the emotion modulated stop-signal task. To evaluate individual differences across decision-making processes involved in inhibitory control, a hierarchical drift-diffusion model was used to fit data from Go-trials for each of the 34 participants. Response threshold in the early processing stage for happy and disgust emotions could be distinguished from the later processing stage at the mid-parietal and mid-frontal regions, respectively, by the single-trial power increments in low frequency (delta and theta) bands. Beta desynchronization in the mid-frontal region was specific for differentiating disgust from neutral emotion in the early as well as later processing stages. The findings are interpreted based on the influence of emotional stimuli on early perceptual processing originating as a bottom-up process in the mid-parietal region and later proceeding to the mid-frontal region responsible for cognitive control processing, which resulted in enhanced inhibitory performance. The results show the importance of mid-frontal and mid-parietal regions in single-trial dynamics of inhibitory control processing.

Keywords: emotion; response inhibition; delta; theta; drift diffusion model

Citation: Nayak, S.; Tsai, A.C. Fronto—Parietal Regions Predict Transient Emotional States in Emotion Modulated Response Inhibition via Low Frequency and Beta Oscillations. *Symmetry* **2022**, *14*, 1244. https://doi.org/10.3390/sym14061244

Academic Editors: Pecchinenda Anna and David A. Becker

Received: 29 March 2022
Accepted: 7 June 2022
Published: 15 June 2022

1. Introduction

We live in an ever-changing environment where rapid motor response and its inhibition play an important role in our survival [1,2]. This ability to implement goal-directed behavior safely is critical; for example, we adjust our movements based on the traffic sign before crossing the street [3]. Motor inhibition is studied in laboratory settings using the stop-signal task (SST) [2] or the Go/NoGo task (GNGT) [4]. The primary objective in a simplified GNGT or SST is a choice reaction task where participants must choose between one of two options and press a button. In GNGT, a percentage of the go-stimulus trials is randomly replaced by a no-go stimulus where the participants are asked not to press a button. In SST some trials are randomly chosen when the Go-stimulus is followed by a stop-stimulus wherein the participants are asked to withhold the ongoing motor response. In short, GNGT is based on action restraint while the stop-signal task relies on the action cancellation [5]. The key difference in GNGT and SST lies in the presentation of the inhibition signal relative to the Go-stimulus (0 ms for the GNGT and ~300 ms for the SST respectively) [6]. This leads to differences in their neural mechanisms leading to motor inhibition. Functional magnetic resonance imaging (fMRI) studies on cognitively healthy human participants highlight functional convergence of these tasks highlighting recruitment of inferior frontal (IFC), (pre-) supplementary motor area (pre-SMA), and/or insular cortex, dorsolateral prefrontal cortex (dfPFC), anterior cingulate cortex (ACC), middle frontal cortex, and posterior parietal regions [7]. SST makes it possible to measure

a behavioral index of stopping by calculating stop-signal reaction time (SSRT) from the reaction time of go-trials and the delay in the stop signal stimulus presentation, referred to as the stop-signal delay (SSD) [8]. This makes SST a more attractive paradigm than GNGT to study motor inhibition in clinical settings since differences in SSRT can be used to account for changes in attention and/or, emotion deficits.

The literature on response inhibition studies can be classified into two categories per se—reactive and proactive inhibition [9,10]. Reactive inhibition is based on action cancellation at the instant of stop signal stimulus presentation. Proactive inhibition necessitates the expectation and planning to stop forthcoming actions when required [11–13]. This anticipation of an approaching stimulus is crucial for goal-directed performance [14,15]. In a response inhibition task, the presence of a stop signal (proactive inhibition) leads to a delay in go trials response as compared to the trials when a stop signal is absent [2,8,16]. Although the fundamental mechanisms by which proactive and reactive inhibition are executed differently, the underlying brain circuitry is similar [17]. The lack of differences in candidate brain regions makes it challenging to study the proactive inhibition [18]. Lately, researchers have tried to study proactive control by measuring decision-making parameter reaction time in Go trials using evidence accumulation models [19–22] and then relating the values to stopping performance. Proactive inhibition has been studied by focusing on the cognitive processes of the stimulus presented in Go-trials as opposed to those in the Stop-trials which is usually done in reactive inhibition studies. This is because the decision-making processes in stopping which determine SSRT can be influenced by the rate of accumulation leading to a correct/incorrect response and the processing speed of the Go-trial stimuli [19,21–23]. Unfortunately, information extracted from the Stop-trials only like SSRT does not tell us anything about the events leading to stopping. In order to extend our current understanding of the decision-making processes in response inhibition leading to stopping, we concentrated on a popular mathematical model used by psychologists for two-choice discrimination tasks called the drift-diffusion model to disentangle reaction time data from SST into relevant decision-making cognitive components as executed in prior studies.

The role of sensory processes has been validated by response inhibition studies in the past [24] and it has been demonstrated in multiple reports that emotional processes take priority to capture attention [25–28]. However, the role of sensory processes in emotion modulated inhibition is still ambiguous. Some studies have suggested that emotions lead to improvement in behavioral inhibition in SST as evident by shorter SSRTs in emotional conditions as opposed to neutral condition [29–31]. Other studies have shown the opposite trend, that is, emotions lead to impairment of behavioral inhibition as evident by longer SSRTs in emotional conditions as opposed to neutral condition [32–36]. Such ambiguous results pose difficulty in interpreting the role of emotion in response inhibition. However, a psychological theory explaining cognitive–emotional interactions [26] helps throw light into the ambiguity in the previous findings. This theory suggests that emotional states can enhance or impair behavioral performance contingent upon their task relevance and that the role of emotions in task performed plays an essential role in the interpretation of the results. When emotions are task-irrelevant or serve as distractors, they lead to poor behavioral performance since they capture attentional resources necessary for the task. On the other hand, when emotions are task-relevant, they lead to improved task performance since they do not compete for attentional resources reserved for cognition.

Previous SST studies based on human scalp electroencephalogram (EEG) studies performing time-frequency analysis report significant enhancement of event-related synchronization power in delta oscillation (1–4 Hz) or theta oscillation (4–8 Hz) bands at frontocentral regions for successful motor inhibition [37]. In addition to this, low-frequency delta/theta oscillatory power is also related to implicit and explicit emotional processing [38]. These findings lead us to predict that low-frequency oscillatory power could play a role in emotion-modulated response inhibition. In our previous report, we showed that low-frequency oscillatory power (LFO; 2–6 Hz) could modulate the response threshold in

favor of emotional conditions relative to neutral conditions at a single-trial level [22]. Additionally, intracranial recordings in human patients [39] as well as multimodal MEG/fMRI approach in healthy human subjects [40] suggest a possible role of beta synchronized power in the right frontal brain regions (right inferior frontal gyrus (IFG)) in line with findings from functional neuroimaging looking at successful inhibition processes. To summarize the previous findings, LFO at middle frontal regions might explain cognitive control processes in response inhibition while beta oscillatory power over the right IFG represents task-specific inhibition in SST.

Speed–accuracy tradeoffs represent a fundamental aspect in cognitive conflict task paradigms like Stroop task, Erikson-Flanker task, GNGT or the SST [41]. Electrophysiology studies on LFO performed in the subthalamic nucleus (STN) (a candidate region for response inhibition as well) suggest that prefrontal–STN connectivity is crucial for speed accuracy tradeoff [42–45]. A recent EEG study in clinically healthy participants reported that changes in cortical LFO power due to speed-accuracy tradeoff are mainly localized in the medial prefrontal cortex (MPFC) [46]. Trial-by-trial changes in LFO power as measured from Fz electrode were shown to be related with activations in MPFC as measured by fMRI. Additionally, signal changes in Fz electrode using EEG and activations in MPFC using fMRI were shown to correlate well with increase in decision thresholds for speed accuracy tradeoff in the same study. These results align well with the notion of so called 'indirect' and 'hyper-direct' pathways for inhibition which recruits subregions of the basal ganglia, thalamus, STN and MPFC [47–49]. Neurobiological models investigating speed–accuracy tradeoffs focus on the basal ganglia and STN since these regions have a wide range of structural and functional connections to cortical (including prefrontal and motor cortex) and subcortical regions of the brain which are involved in decision-related processes [50].

Evidence accumulation models like the drift-diffusion model (DDM) and Linear ballistic accumulator (LBA) [51] belong to a class of formal computational models which have been developed to fit the biologically plausible and experimentally robust manipulations of cognition. Lately, these models have been shown to be useful in a task general setting to study individual differences in clinical neuroscience [52]. By accounting for individual differences, we will be able to make better inferences in psychopathology and their causal links to neurobiology. The role of the emotional content in response inhibition is not clear [53] and we hope our findings will add on to this literature on evidence accumulation studies.

A majority of EEG studies have focused on frontocentral N2 and P3 event-related potentials (ERPs) for understanding reactive inhibition owing to the presence of both these components in GNGT and SST [37,54,55]. In contrast, studies involving proactive inhibition have looked at trial-by-trial changes in inferoposterior N1, an earlier ERP component believed to capture attention [20,21,56]. Task-relevant stopping led to smaller N1 amplitudes for longer reaction times, indicating that proactive inhibition captures information related to selective attentional processes [20] unlike being associated with global stopping like the P3 component, as evaluated by reactive inhibition [57,58]. In order to obtain a complete view of proactive inhibition, we added the mid-parietal region in addition to the mid-frontal region to look at dynamic changes in the amplitude of the frequency spectrum as a function of time from Go trials responsible for decision-making processes.

In this current study, the impact of task-relevant emotions in action cancellation was investigated in more detail. We hypothesized that transient affective states would enhance response inhibition both at behavioral as well as neural levels. We predicted that emotional conditions would show shorter response times in go as well as stop trials. At the neural level, we expected that lower frequency oscillatory activity in delta and theta band could distinguish response threshold for emotional relative to neutral condition owing to previous literature supporting evidence of delta/theta activity in emotional processes and inhibitory control. Since emotion is better understood as a bottom-up process and proactive studies in the past have focused on the inferoposterior N1 ERP component, so we included the mid-parietal region in addition to the frontal scalp site to understand the

role of emotion perception in response inhibition. In addition, we conducted exploratory analyses in frontal and posterior regions to look at the role of beta oscillatory power in motor inhibition. To relate oscillatory power with decision-making processes, we combined single-trial oscillatory activity from the delta, theta, and beta frequency bands in frontal and posterior scalp sites with drift-diffusion parameters obtained from Go-trials across emotional (disgust/happy) and neutral conditions. Subsequently, we used within-subject regression analysis to map out specific links between changes in trial-by-trial oscillatory activity and emotional conditions.

2. Materials and Methods

2.1. Participants

Thirty-four young participants (9 females; mean age: 24.35 years; SD: 3.88 years) were recruited for this experiment. All subjects were right-handed and had no previous history of psychological or neurological disorders. All methods were carried out following relevant guidelines and regulations with the Human Research Ethics Committee IRB on Biomedical Science Research /IRB-BM Academia Sinica, Taiwan, based on the tenets of the Declaration of Helsinki. All experimental protocols used in this study followed the relevant guidelines imposed by the Human Research Ethics Committee IRB on Biomedical Science Research/IRB-BM Academia Sinica, Taiwan. All subjects signed consent forms in agreement with the Human Research Ethics Committee IRB on Biomedical Science Research/IRB-BM Academia Sinica, Taiwan. None of the participants claimed to have participated in a similar research study previously. One participant was removed due to a lot of artifacts in the recording data. The results presented in the current article are from the remaining 33 participants. Although a formal power analysis for the sample size was not conducted for this study, the sample size used here was in line with other evidence accumulation studies in the literature [19,43,59,60].

2.2. Material and Experimental Design

The experiment was performed in an echo-proof diffusely lit room wherein participants were asked to be seated at ease. Visual stimuli were depicted on a computer monitor having dimensions of 24.4 $\times$ 18.3 cm positioned 60 cm in front of the participants. The participants were given instructions to perform a series of choice reaction tasks while electroencephalography was used for recording the electrical activity of their brains. The overall experiment was based on an A-B-A-B block design. Block A used SST with disgust and neutral faces as target images, while block B used happy and neutral faces. Participants were switched between assignments of blocks A and B to nullify the bias in findings across subjects. The experiment design is displayed in Figure 1.

Every trial commenced with a fixation cross for 500 ms, succeeded by the presentation of an emotional face for 1000 ms and a blank screen which served as an inter-trial interval (ITI). The ITI was jittered between 1–1.5 s. For the Go trials, subjects had to respond by pressing a button on the keyboard within 1 s of the picture shown identifying the type of face presented to them: happy, disgust, or neutral. Participants had to press the "Z" or "M" buttons on the keyboard for correct recognition of emotional or neutral faces respectively. In approximately 28% of the trials, the Go trial was followed by a red border around the same stimulus to act as a stop trial. The red border's latency was jittered in accordance with the participant's task performance in the current trial for making the stop trials unpredictable. The participants were instructed to press a previously assigned response button on the keyboard ("Z" or "M") as soon as they could without worrying too much about making errors in stop trials. The stop-signal delay (SSD) was set to 250 ms initially. The SSD on the succeeding stop trial was reduced by 50 ms to make it easier on participants if they were incapable of stopping successfully in the current stop trial. On the contrary, the SSD was increased by 50 ms on the succeeding stop trial to make it harder for the participant to stop his/her ongoing motor movements if they were capable of stopping successfully in the current stop trial. This was to ensure that the hit rate in the stop trials would hover

around the 50% mark. The trials were equally divided among two emotion conditions—happy/disgust faces and neutral faces trials. In total, participants were presented with 100 Go trials and 40 Stop trials for every emotion category respectively spanning two blocks. The emotional faces were chosen from a Taiwanese face database [61] to prevent conclusions on a cultural bias of the faces presented to participants. The closed-mouth images were used for disgusting, happy, and neutral trials. The emotional SST design used in the current study was adapted from a previously published functional magnetic resonance imaging (fMRI) research [30]. All the faces chosen were grey scaled to a particular size (506 × 650 pixels; 96 dpi) and oval masked with a black background to prevent the impact of spatial properties. This was done to prevent bottom-up stimulus-driven biases for the participant's button presses.

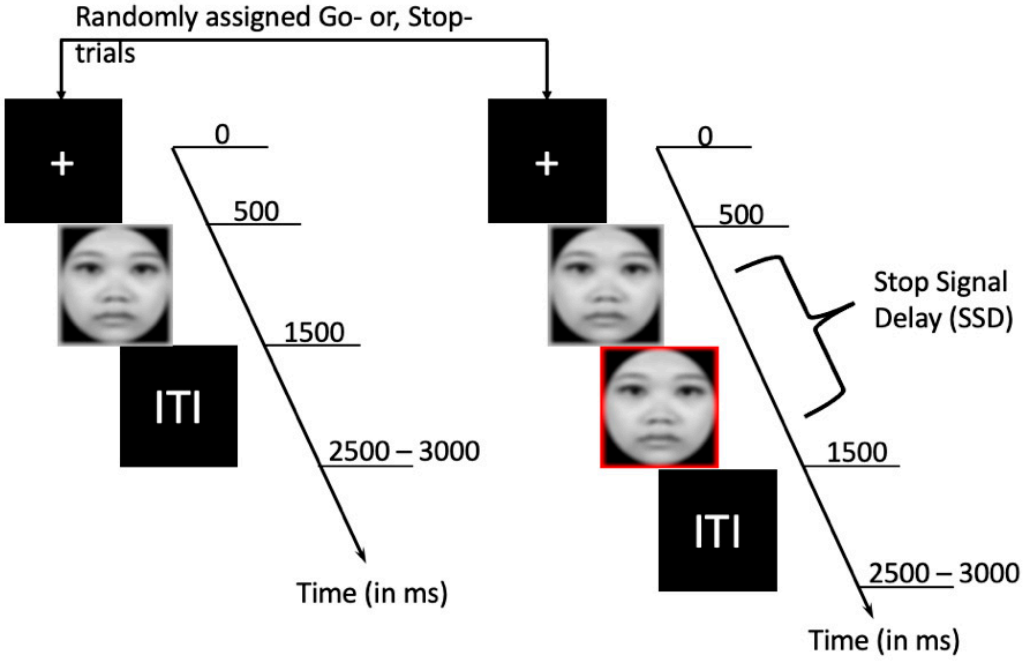

Figure 1. Study design for the emotional stop-signal task used in the current study. Participants were asked to respond to emotional faces as quickly as possible without using any inherent strategy to obtain a correct response. The faces were morphed with a grey border to signal as a Go-trial. On some trials, the grey border changed to red border to signal as a stop signal. Participants were instructed to try to inhibit their response upon seeing the stop signal. Initial stop-signal delay (SSD) was set to 250 ms.

2.3. Data Collection and Analyses

2.3.1. EEG Recording

Electroencephalography (EEG) recording was performed by placing 128 Ag/AgCl electrodes on the participant's scalp. This included six facial electrodes. The reference was placed in between the Fz and Cz electrode sites based on the 10–20 electrode system. Three electrodes were placed around both eyes in order to control eye movements during the scan. The changes in heart rate were accessed by placing an electrode near the index finger of both hands. The data obtained from eye movements and heart rate electrodes were regressed out as covariates in subsequent analysis. To ensure good SNR, electrode impedances were kept below 20 kΩ throughout the experiment. The EEG signals were amplified using Neuroscan amplifiers having an analog bandpass of 0.1–100 Hz. The sampling frequency used was 1000 Hz.

2.3.2. EEG Analysis

Time-domain analyses were carried out using EEGLAB Version 14.1.2b [62], an open-source toolbox running under MATLAB environment. Custom written scripts were used to remove bad channels and epochs after setting a baseline of 200 ms (200 ms before picture showing for Go trials was used for baseline calculation for Go and Stop trials). Baseline correction was done for disgust/happy and neutral emotions across Go and Stop conditions separately. Artifacts were removed by performing the independent component analysis (ICA) on all trials for each subject individually. The overall clean data resulted in 85 successful Go trials and 24 successful Stop trials on average across three emotion conditions. Bandpass filtering was done between 1 to 50 Hz to avoid spectral contamination of EEG data from a line frequency of 60 Hz. Epoch length was restricted to 2700 ms for each trial, including 1200 ms before picture showing and 1500 ms after post-stimulus onset. Trials in the "Go" and "Stop" condition having missing values or trials with peak-to-peak amplitude differences of more than 100 μV were excluded from the analysis.

Event-related spectral perturbations (ERSPs) at the single-trial level [63] were calculated using the *pop_newtimef* function by including 2700 ms of filtered epoch data (including 1200 ms before picture showing). The data from 33 participants were averaged to generate group-level ERSP. In line with previous studies [22,45], data from the Fz electrode scalp site was used to proxy the mid-frontal region. In a similar vein, data from the Pz electrode scalp site was used to proxy the mid-parietal region. Go- and Stop-signal ERSPs were calculated independently for each category of emotion condition: disgust, happy and neutral, all adjusted to the 200 ms baseline defined in the pre-stimulus period. We extracted 200 frequencies spanning from 1.0 to 50.0 Hz in the linear scale and used a fixed window size of 256 ms (256 samples). ERSP results were analyzed for three different frequency bands (delta (1–4 Hz), theta (4–8 Hz), and beta (15–30 Hz)) and two-time windows (early (0–300 ms) and late (300–600 ms)) respectively. The time windows were chosen to keep the values of SSRT (~ 320 ms) and average Go-trial reaction time (~675 ms) in mind. These time windows overlap well with the time windows occupied by the prominent ERP and components N2/P3 used in the inhibition literature [37,64]. In addition, time windows used for delta/theta frequency bands by the few ERSP studies on response inhibition also overlap with the time windows we have chosen for analysis in the current study. We calculated single-trial ERSP also by the *pop_newtimef* function. The baseline for single trials was set from −200 to 0 ms prior to stimulus onset and single-trial stimulus-locked ERSP was estimated separately for delta, theta, and beta frequency bands by subtracting this information from the relevant trials in each condition. The single-trial ERSPs were normalized for theta, delta, and beta frequency bands separately by dividing their respective baseline power values in each trial. This approach has been shown to provide more robust estimates for the single-trial power [63].

2.3.3. Hierarchical Drift Diffusion Model (HDDM) Analysis

Trial-by-trial dynamics of decision-making components as given by the drift-diffusion model (DDM) [65], we used the hierarchical drift-diffusion model package version 0.6.0 (HDDM) [66] which used Bayesian estimation for modeling DDM parameters. Go trial reaction times (Go RTs) were used as done so in previous articles using DDM analysis [19,23] for SST across happy, disgust, and neutral conditions. There were two possible responses for successful or failed emotion recognition (here, we choose accuracy coding where 1 means the subject successfully identified the correct emotional facial expression, and 0 means the subject pressed the incorrect button). Model comparison was done using the deviance information criterion (DIC). A combination of the three DDM parameters—level of response caution (response threshold, $\boldsymbol{a}$), evidence accumulation (drift rate, $\boldsymbol{v}$), and time needed for non-decision processes (non-decision time, $\boldsymbol{t_0}$) was used to define three models in order to determine the impact of visual affect (happy, disgust or neutral) on choice RT obtained by Go trials. First, a set of stimulus-varying models were inspected by varying two or more DDM parameters across different stimulus conditions (Disgust stimulus, DS; Happy

stimulus, HS; and Neutral stimulus, NS). After that, two regression models were used to capture dynamics in low frequency oscillatory and beta power varying with trial-by-trial reaction time. The regression coefficients for mid-frontal and mid-parietal activity decision thresholds were further used to determine the decision-making parameters themselves in the same model. The response threshold, a in a given trial was defined as follows

$$a = b_0 + b_1\, delta * Stim + b_2\, theta * Stim + b_3\, beta * Stim,$$

where, Stim indicates the type of stimulus used (DS, HS, or NS), delta/theta refers to the post-stimulus increment in the power of the delta/theta frequency bands, beta refers to the post-stimulus decline in the power of the beta frequency band, and b_{1-3} are the estimated regression coefficients. Further modeling details have been explained in Appendix A.

HDDM uses a Markov chain Monte Carlo (MCMC) to obtain a sequence of samples from the posterior of each parameter for each model. We generated 10,000 samples from the posteriors for model convergence for all models used in the current study. The first 2000 samples were thrown out as "burn-in" to ensure that the MCMC samples used came from a stationary distribution. The readers are referred to the other references [19,23] for further modeling details. We discarded 5% of the data to prevent outliers, assuming that the DDM process might not generate 5% of the data but instead by attentional lapses. Posterior probabilities of the DDM parameters having values greater than or equal to 95% different from zero were considered as significant [43]. Model comparison was based on the deviance information criterion (DIC) values. A model is considered to be significantly different from models if the difference in DIC values is greater than 10 [43].

2.3.4. Statistical Analysis

The median RT values for the Go trials were calculated across each emotion condition separately after excluding the error trials. SSRT was estimated for the disgust, happy and neutral emotion conditions separately after accounting for the Go-trial omissions using the integration method [16]. Paired t-test analyses were used to test how emotion modulated behavioral performance in go and stop trials. For the ERSP analysis, repeated-measures ANOVA was used to test how emotion modulated neural activity in delta, theta, and beta oscillatory bands across mid-frontal and mid-parietal scalp sites.

3. Results

3.1. Behavioral Results

The behavioral results showed that participants made faster responses to disgust ($t(32) = -2.646$, $p = 0.013$) and happy ($t(31) = -3.696$, $p = 0.001$) conditions relative to neutral condition in Go trial reaction times (RTs). The same trend was seen in Stop trials (Stop signal reaction times, SSRTs) for the disgust ($t(32) = -2.004$, $p = 0.054$) as well as happy ($t(31) = -2.747$, $p = 0.010$) condition relative to the neutral condition. The behavioral results are presented in Table 1.

Table 1. Mean and standard deviation of reaction time in Go and Stop trials for the negative and positive block.

	Go Reaction Time (RT)	Stop Signal Reaction Time (SSRT)
Negative block		
Disgust	672.5 ± 99.3	313.7 ± 56.6
Neutral	689.7 ± 95.0	327.8 ± 55.1
Positive block		
Happy	662.5 ± 110.0	309.9 ± 59.7
Neutral	680.2 ± 99.1	321.8 ± 49.41

Reaction times in milliseconds are given by M ± SD.

3.2. Linking DDM Parameters with Behavior Data

The best-fitting model parameters were used to probe into the neural oscillatory processes involved in emotion modulation of inhibitory control. To understand how well the model parameters fit the behavioral results in go and stop trials, we present correlation matrices in Tables 2 and 3 for disgust and happy emotion block, respectively. The DDM parameters derived from Go trials (as denoted by DDM_a, DDM_v, DDM_t_0 for response threshold, drift rate, and non-decision time components, respectively) were well correlated with behavioral measures derived from go and stop trials, suggesting that indirect inferences can be made on inhibitory control using information derived from Go trials only.

Table 2. Correlation matrix for behavioral measures in disgust block.

		Disgust Go DDM_a	**Neutral Go DDM_a**	**Disgust Go DDM_v**	**Neutral Go DDM_v**	**Disgust Go DDM_t_0**	**Neutral Go DDM_t_0**
Disgust Go RT	Correlation	0.872 **	0.814 **	−0.671 **	−0.534 **	0.517 **	0.405 *
	Sig. (2-tailed)	0.000	0.000	0.000	0.001	0.002	0.019
Neutral Go RT	Correlation	0.749 **	0.824 **	−0.700 **	−0.609 **	0.409 *	0.451 **
	Sig. (2-tailed)	0.000	0.000	0.000	0.000	0.018	0.008
Disgust Stop SSRT	Correlation	0.762 **	0.641 **	−0.670 **	−0.472 **	0.274	0.319
	Sig. (2-tailed)	0.000	0.000	0.000	0.006	0.123	0.070
Neutral Stop SSRT	Correlation	0.364 *	0.498 **	−0.640 **	−0.511 **	−0.037	0.245
	Sig. (2-tailed)	0.037	0.003	0.000	0.002	0.839	0.169

* Correlation is significant at the 0.05 level (2-tailed). ** Correlation is significant at the 0.01 level (2-tailed).

Table 3. Correlation matrix for behavioral measures in happy block.

		Happy Go DDM_a	**Neutral Go DDM_a**	**Happy Go DDM_v**	**Neutral Go DDM_v**	**Happy Go DDM_t_0**	**Neutral Go DDM_t_0**
Happy Go RT	Correlation	0.929 **	0.892 **	−0.329	−0.570 **	0.628 **	0.475 **
	Sig. (2-tailed)	0.000	0.000	0.066	0.001	0.000	0.006
Neutral Go RT	Correlation	0.894 **	0.922 **	−0.311	−0.551 **	0.635 **	0.550 **
	Sig. (2-tailed)	0.000	0.000	0.083	0.001	0.000	0.001
Happy Stop SSRT	Correlation	0.686 **	0.713 **	−0.413 *	−0.576 **	0.415 *	0.242
	Sig. (2-tailed)	0.000	0.000	0.019	0.001	0.018	0.181
Neutral Stop SSRT	Correlation	0.564 **	0.668 **	−0.349 *	−0.496 **	0.368 *	0.313
	Sig. (2-tailed)	0.001	0.000	0.050	0.004	0.038	0.081

* Correlation is significant at the 0.05 level (2-tailed). ** Correlation is significant at the 0.01 level (2-tailed).

3.3. Exploring Trial-by-Trial Regression Analysis of ERSP Data with DDM Parameters

To understand the link between trial-by-trial variations in oscillatory activity and DDM parameters, we ran regression analyses using the HDDM package. For the early time window (0–300 ms), trial-by-trial variations in beta power from the mid-frontal region decreased the estimated response threshold for disgust (98% posterior probability) (Figure 2a) and happy (96% posterior probability) (Figure 2b) emotion as opposed to neutral emotion. The same effect failed to reach significance for theta or delta power. For the mid-parietal region, trial-by-trial changes in delta power increased the estimated response threshold parameter for disgust (97% posterior probability) (Figure 2c) and happy (96% posterior probability) (Figure 2d) emotion as opposed to neutral emotion. In addition, changes in theta (100% posterior probability) (Figure 2d) as well as beta (100% posterior probability) (Figure 2d) power from the mid-parietal for happy emotion, as opposed to the neutral emotion, affected the response threshold parameter.

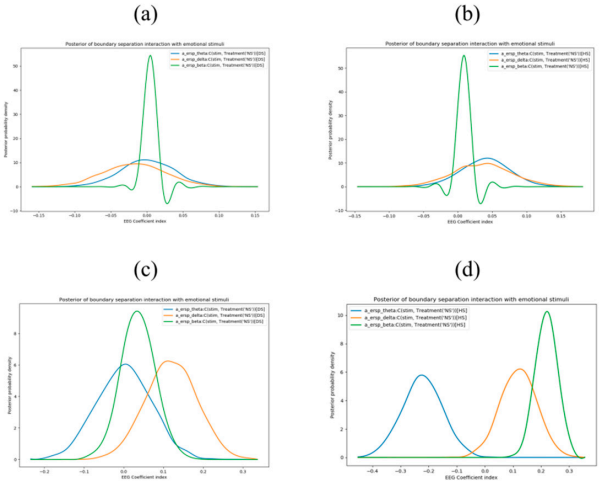

Figure 2. Single-trial ERSP associated with delta, theta, and beta power for disgust, happy and neutral stimuli in the early time stage (0–300 ms). In the figures on the left (**a**,**c**), posterior probability density reflects the decision threshold increase for disgust relative to the neutral context in mid-frontal and mid-parietal regions, respectively. In the figures on the right (**b**,**d**), posterior probability density reflects the decision threshold increase for the happy relative to the neutral context in mid-frontal and mid-parietal regions respectively.

We also ran exploratory analyses in the later time window (300–600 ms). Trial-by-trial variations in delta and theta power from the mid-frontal region affected the estimated response threshold for disgust (95% posterior probability; 98% posterior probability) (Figure 3a) and happy (100% posterior probability; 100% posterior probability) (Figure 3b) emotion relative to neutral emotion. In addition, changes in beta (96% posterior probability) power from the mid-frontal region affected the response threshold parameter for disgust emotion as opposed to neutral emotion. For the mid-parietal region, changes in delta and theta power affected the estimated response threshold for happy (99% posterior probability; 97% posterior probability) (Figure 3d) emotion relative to neutral emotion. No such effects were observed for disgust compared to neutral emotion (Figure 3c).

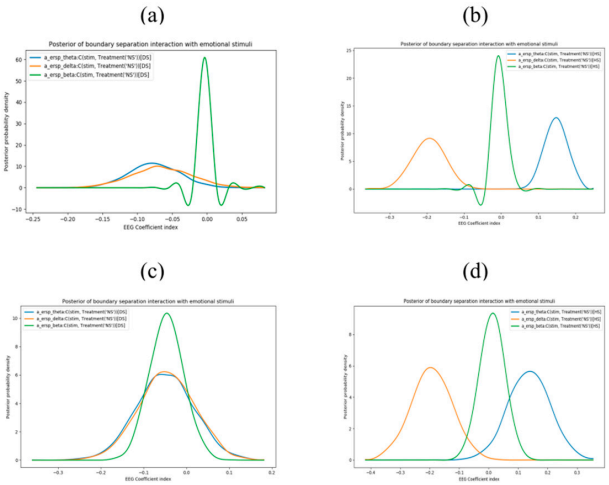

Figure 3. Single-trial ERSP associated with delta, theta, and beta power for disgust, happy and neutral stimuli in the later processing stage (300–600 ms). In the figures on the left (**a**,**c**), posterior probability density reflects the decision threshold increase for disgust relative to the neutral context in mid-frontal and mid-parietal regions respectively. In the figures on the right (**b**,**d**), posterior probability density reflects the decision threshold increase for happy relative to the neutral context in mid-frontal and mid-parietal regions respectively.

4. Discussion

The present study examined the impact of task-relevant emotions in inhibitory control at the behavioral and neural levels. We found that oscillatory dynamics derived from single-trial EEG recordings predicted transient emotional states in emotion modulated response inhibition tasks. Emotional faces were associated with faster response times in both go and stop trials relative to neutral faces, suggesting that task-relevant emotion improved response inhibition [30]. A recent study [67] has shown that positive emotion enhances response inhibition in the elderly when emotion is task-relevant. The current study showed that both positive and negative emotion could enhance response inhibition when emotion is task-relevant, as evidenced by shorter SSRTs in emotional conditions relative to neutral conditions, confirming our hypothesis in line with the dual competition framework [26]. In addition, the behavioral data support a previous report investigating cognitive-emotional interactions in response inhibition showing faster responses for happy and fearful trials as compared to neutral trials [29].

The current results extend the findings from our previous study [22], wherein we sought to establish the role of low-frequency oscillatory power in emotion modulated response inhibition. Here, we showed that trial-by-trial changes in delta power modulated response threshold in favor of happy and disgust affect compared to neutral affect in the early time window at the mid-parietal region but not the mid-frontal region. However, in the later time window, trial-by-trial changes in delta and theta power helped enhance the happy and disgust affect compared to neutral affect at mid-frontal but not mid-parietal regions. This extends previous reports on the role of delta and theta oscillations in implicit and explicit emotion recognition [38]. Previous studies have associated an escalation in delta and theta synchronizations at the mid-frontal region with the inhibitory control [37]. The results from the current study replicate this effect. In addition, the results show that cognitive changes associated with delta and theta power are better understood with different temporal processing stages. Emotion perception can be understood by bottom-up processes manifesting in the mid-parietal region (from stimulus showing to under 300 ms after picture showing) and later in the mid-frontal region (after 300 ms after picture showing) [68]. The results hold relevance for the emotion modulated stopping process since the SSD measured in the current study was around 300 ms for disgust and happy emotion. We suggest that the trial-by-trial enhancements in delta/theta power obtained in the mid-frontal region after 300 ms post-stimulus presentation reflect cognitive control processes associated with decision-making processes since, the mean RT in Go trials was around 700 ms in the current study. The latency of the time windows for these findings are in line with a recent study which analyzes the role of right IFG in response inhibition initiation and stopping performance (mean of successful stop SSD was 288 ms and stopping performance was analyzed from a window of 100–350 ms from Stop stimulus presentation) [40].

Response threshold was positively correlated with Go RT and SSRT, suggesting that speed-accuracy tradeoff in Go trials could be linked with better inhibitory performance [19,21,23] across disgust, happy and neutral emotions. Interestingly, subjects whose Go trials were marked with a more substantial drift rate also had shorter SSRTs for disgust, happy and neutral emotions, suggesting that they were better at inhibiting their responses. A previous SST study also obtained similar results on the drift rate and response threshold parameters [23]. The non-decision parameter mainly reflects individual differences in motor execution and periods of inattention before attending a stimulus, so finding no significant correlations with this parameter and SSRT measures was expected as in previous studies. A significant correlation between SSRT derived from happy and neutral stop trials and non-decision parameters derived from the happy Go trial was obtained, which was unexpected. We reason that happy affect might be similar to the neutral affect shown for many participants so inattention in this emotion category was related to the behavioral inhibition!

Increased decision thresholds were observed for emotional relative to the neutral condition associated with trial-by-trial variations in delta and theta power over the mid-frontal region. A well-established finding for LFO power increase in STN is commonly

observed in electrophysiology studies and it is shown to be related to the prefrontal–STN connectivity [42,46]. The mid-frontal region has structural and functional connections to the STN as demonstrated in previous studies [47,48]. The prefrontal cortex intensifies its impact over the STN with an increase in task complexity resulting in longer decision thresholds for response. The emotion modulated motor inhibition task used in this study can be visualized as an adaptive speed–accuracy tradeoff task since participants were required to focus on responding as quickly as possible to the salient emotional stimuli as part of their instructions without thinking much about the accuracy of their responses. To sum up, it would be too impulsive to conclude that cortical LFO changes from EEG scalp-based studies follow a simple one-to-one mapping; since LFO activity over the PFC has been associated with several other cognitive processes, including novelty, error, punishment, emotional reactivity, learning, and memory [44,69].

A recent study attributes improved stopping performance to an increase in beta oscillatory power initiated from the right IFG [40]. We found that trial-by-trial beta power could differentiate disgust emotion from neutral emotion in the midfrontal region in the early as well as late time window (0~600 ms). This could imply a generalized role for beta oscillations in the inhibitory control task. Based on the findings observed in the current study, one might infer that the variations in beta power in the early processing stage at mid-frontal regions are crucial for differentiating disgust and happy emotion compared to neutral emotion. These results fit well with the findings of emotional faces capturing additional attentional resources [25,27], and changes in the beta frequency band might help better understand them. However, inconsistencies in the variations of beta power in happy and disgust emotions for early and later processing stages make it hard for us to conclude the role of beta oscillations in emotional inhibition at a trial-by-trial level. Future reports could look at interactions between LFO and beta power in the mid-frontal region to better understand the role of single-trial beta oscillations in cognitive control tasks.

The study has a few limitations. Firstly, DDM is not the only approach to model SST. Usage of DDM in response inhibition must be evaluated carefully in realistic experiment designs as concluded by experts in the field [70]. Alternative methods like the dynamic models of choice (DMC) [51] allow more flexibility with a hands-on approach concerning the models used. However, DMC's implementation is not straightforward, and it can be a little demanding for the end-user. Secondly, the current study only focused on happy and disgusted faces. So, the results are not generalizable to other emotion categories and thus must be interpreted with caution in the future. Finally, we demonstrated trial-by-trial changes from only two regions owing to computational and time constraints on the model convergence. Although the use of only two sensors seems somewhat biased and an average of electrodes around the aforementioned electrode sites (Fz and Pz) would seem to improve the generalizability of the findings, previous EEG literature from normal healthy subjects and Parkinson patients [43,71] have reported findings from these electrode sites and we were merely trying to replicate the findings for response inhibition. In particular, the finding of theta power for FCz/Fz electrode is robust so it was used for lower frequency oscillations. Future studies are recommended to extend this framework to the rest of the brain and use a standard atlas in MNI space to explain emotion modulated response inhibition in a better manner by considering brain's asymmetry as well.

5. Conclusions

In summary, the results provide insight into the relationship between decision-making components and oscillatory activity underlying task-relevant emotions in response inhibition. The results show that the response threshold parameter is associated with changes in delta power over occipital regions in the early perceptual window and with delta and theta power over the frontal region in the later processing stage. These findings highlight a close relationship between inhibitory processing and response threshold at the neural level in frontal and parietal regions. The model-based approach offers a crucial understanding of the interactions between decision-making components involved in inhibitory control.

Although we focused on midline regions, the interaction of inhibitory control processes with sensory stimulations (visual/auditory) involves several cognitive processes that are based on brain asymmetry and need to be dealt with care. It raises thought-provoking inquiries about strategic modifications in inhibitory performance coupled with neuropsychiatric ailments like attention deficit hyperactivity disorder (ADHD), Parkinson's disease, and obsessive-compulsive disorder (OCD). A recent review [52] on usage of evidence accumulation models as a tool to measure cognitive differences in clinical neuroscience has been proposed which extends the discussions in the current article.

Author Contributions: Conceptualization, S.N. and A.C.T.; Data curation, S.N. and A.C.T.; Formal analysis, S.N.; Funding acquisition, A.C.T.; Investigation, S.N. and A.C.T.; Methodology, S.N.; Project administration, A.C.T.; Resources, A.C.T.; Software, S.N.; Supervision, A.C.T.; Validation, S.N.; Visualization, S.N.; Writing—original draft, S.N.; Writing—review & editing, S.N. and A.C.T. All authors have read and agreed to the published version of the manuscript.

Funding: This research was funded by the Ministry of Science and Technology (MOST), Taiwan grant number MOST 110-2118-M-001-006-MY2, and The APC was funded by MOST 110-2118-M-001-006-MY2.

Institutional Review Board Statement: The study was conducted in accordance with the Declaration of Helsinki and approved by the Human Research Ethics Committee IRB on Biomedical Science Research/IRB-BM Academia Sinica, Taiwan with the approval number AS-IRB-BM-16045 and the date of approval was 2016-11-09.

Informed Consent Statement: Informed consent was obtained from all subjects involved in the study.

Data Availability Statement: The data used to support the findings of this study are available from the corresponding author upon reasonable request.

Acknowledgments: The authors would like to appreciate the commitment of all participants of this study and thank MOST for funding the current research.

Conflicts of Interest: The authors declare no conflict of interest. The funders had no role in the design of the study; in the collection, analyses, or interpretation of data; in the writing of the manuscript, or in the decision to publish the results.

Appendix A

We provide some HDDM modelling details to help explain how posteriors relative to neutral condition were modelled in the model shown in the main text.

(1) For the within-subject regression model of behavior data, the model used was

$$model = hddm.HDDMRegressor(data, \{\text{“}a \sim C(stim, Treatment(\text{‘}NS\text{’}))\text{”}, \text{“}v \sim C(stim, Treatment(\text{‘}NS\text{’}))\text{”}, \text{”}t \sim C(stim, Treatment(\text{‘}NS\text{’}))\text{”}\}, p\_outlier = 0.05)$$

(2) For the neural regression models, the model used was

$$model = hddm.HDDMRegressor(data, \{\text{“}a \sim C(stim, Treatment(\text{‘}NS\text{’})) + ersp\_theta + ersp\_theta : C(stim, Treatment(\text{‘}NS\text{’})) + ersp\_delta + ersp\_delta : C(stim, Treatment(\text{‘}NS\text{’})) + ersp\_beta + ersp\_beta : C(stim, Treatment(\text{‘}NS\text{’}))\text{”}\}, p\_outlier = 0.05)$$

Here, C (stim, Treatment('NS') was used to model the posteriors for happy and disgust stimuli against the neutral stimuli in both the models.

References

1. Diamond, A. Executive functions. *Annu. Rev. Psychol.* **2013**, *64*, 135–168. [CrossRef] [PubMed]
2. Logan, G.D.; Cowan, W.B. On the ability to inhibit thought and action: A theory of an act of control. *Psychol. Rev.* **1984**, *91*, 295. [CrossRef]
3. Dutra, I.C.; Waller, D.A.; Wessel, J.R. Perceptual surprise improves action stopping by nonselectively suppressing motor activity via a neural mechanism for motor inhibition. *J. Neurosci.* **2018**, *38*, 1482–1492. [CrossRef]
4. Donders, F.C. On the speed of mental processes. *Acta Psychol.* **1969**, *30*, 412–431. [CrossRef]
5. Schachar, R.; Logan, G.D.; Robaey, P.; Chen, S.; Ickowicz, A.; Barr, C. Restraint and cancellation: Multiple inhibition deficits in attention deficit hyperactivity disorder. *J. Abnorm. Child Psychol.* **2007**, *35*, 229–238. [CrossRef]
6. Raud, L.; Westerhausen, R.; Dooley, N.; Huster, R.J. Differences in unity: The go/no-go and stop signal tasks rely on different mechanisms. *NeuroImage* **2020**, *210*, 116582. [CrossRef]
7. Aron, A.R.; Durston, S.; Eagle, D.M.; Logan, G.D.; Stinear, C.M.; Stuphorn, V. Converging evidence for a fronto-basal-ganglia network for inhibitory control of action and cognition. *J. Neurosci.* **2007**, *27*, 11860–11864. [CrossRef]
8. Verbruggen, F.; Logan, G.D. Response inhibition in the stop-signal paradigm. *Trends Cogn. Sci.* **2008**, *12*, 418–424. [CrossRef]
9. Van Belle, J.; Vink, M.; Durston, S.; Zandbelt, B.B. Common and unique neural networks for proactive and reactive response inhibition revealed by independent component analysis of functional MRI data. *Neuroimage* **2014**, *103*, 65–74. [CrossRef]
10. Aron, A.R. From reactive to proactive and selective control: Developing a richer model for stopping inappropriate responses. *Biol. Psychiatry* **2011**, *69*, e55–e68. [CrossRef]
11. Chikazoe, J.; Jimura, K.; Hirose, S.; Yamashita, K.-I.; Miyashita, Y.; Konishi, S. Preparation to inhibit a response complements response inhibition during performance of a stop-signal task. *J. Neurosci.* **2009**, *29*, 15870–15877. [CrossRef] [PubMed]
12. Vink, M.; Kaldewaij, R.; Zandbelt, B.B.; Pas, P.; du Plessis, S. The role of stop-signal probability and expectation in proactive inhibition. *Eur. J. Neurosci.* **2015**, *41*, 1086–1094. [CrossRef] [PubMed]
13. Zandbelt, B.B.; Vink, M. On the role of the striatum in response inhibition. *PLoS ONE* **2010**, *5*, e13848. [CrossRef] [PubMed]
14. Braver, T.S. The variable nature of cognitive control: A dual mechanisms framework. *Trends Cogn. Sci.* **2012**, *16*, 106–113. [CrossRef] [PubMed]
15. Critchley, H.D.; Mathias, C.J.; Dolan, R.J. Neural activity in the human brain relating to uncertainty and arousal during anticipation. *Neuron* **2001**, *29*, 537–545. [CrossRef]
16. Verbruggen, F.; Aron, A.R.; Band, G.P.; Beste, C.; Bissett, P.G.; Brockett, A.T.; Brown, J.W.; Chamberlain, S.R.; Chambers, C.D.; Colonius, H. A consensus guide to capturing the ability to inhibit actions and impulsive behaviors in the stop-signal task. *eLife* **2019**, *8*, e46323. [CrossRef]
17. Zhang, F.; Iwaki, S. Common neural network for different functions: An investigation of proactive and reactive inhibition. *Front. Behav. Neurosci.* **2019**, *13*, 124. [CrossRef]
18. Verbruggen, F.; Logan, G.D. Proactive adjustments of response strategies in the stop-signal paradigm. *J. Exp. Psychol. Hum. Percept. Perform.* **2009**, *35*, 835. [CrossRef]
19. Jahfari, S.; Ridderinkhof, K.R.; Scholte, H.S. Spatial frequency information modulates response inhibition and decision-making processes. *PLoS ONE* **2013**, *8*, e76467. [CrossRef]
20. Langford, Z.D.; Krebs, R.M.; Talsma, D.; Woldorff, M.G.; Boehler, C.N. Strategic down-regulation of attentional resources as a mechanism of proactive response inhibition. *Eur. J. Neurosci.* **2016**, *44*, 2095–2103. [CrossRef]
21. Langford, Z.D.; Schevernels, H.; Boehler, C.N. Motivational context for response inhibition influences proactive involvement of attention. *Sci. Rep.* **2016**, *6*, 35122. [CrossRef]
22. Nayak, S.; Kuo, C.; Tsai, A.C.-H. Mid-Frontal Theta Modulates Response Inhibition and Decision Making Processes in Emotional Contexts. *Brain Sci.* **2019**, *9*, 271. [CrossRef]
23. White, C.N.; Congdon, E.; Mumford, J.A.; Karlsgodt, K.H.; Sabb, F.W.; Freimer, N.B.; London, E.D.; Cannon, T.D.; Bilder, R.M.; Poldrack, R.A. Decomposing decision components in the stop-signal task: A model-based approach to individual differences in inhibitory control. *J. Cogn. Neurosci.* **2014**, *26*, 1601–1614. [CrossRef]
24. Booth, J.R.; Burman, D.D.; Meyer, J.R.; Lei, Z.; Trommer, B.L.; Davenport, N.D.; Li, W.; Parrish, T.B.; Gitelman, D.R.; Mesulam, M.M. Neural development of selective attention and response inhibition. *Neuroimage* **2003**, *20*, 737–751. [CrossRef]
25. Vuilleumier, P. How brains beware: Neural mechanisms of emotional attention. *Trends Cogn. Sci.* **2005**, *9*, 585–594. [CrossRef]
26. Pessoa, L. How do emotion and motivation direct executive control? *Trends Cogn. Sci.* **2009**, *13*, 160–166. [CrossRef]
27. Pourtois, G.; Schettino, A.; Vuilleumier, P. Brain mechanisms for emotional influences on perception and attention: What is magic and what is not. *Biol. Psychol.* **2013**, *92*, 492–512. [CrossRef]
28. Pessoa, L.; Kastner, S.; Ungerleider, L.G. Attentional control of the processing of neutral and emotional stimuli. *Cogn. Brain Res.* **2002**, *15*, 31–45. [CrossRef]
29. Pessoa, L.; Padmala, S.; Kenzer, A.; Bauer, A. Interactions between cognition and emotion during response inhibition. *Emotion* **2012**, *12*, 192. [CrossRef]
30. Pawliczek, C.M.; Derntl, B.; Kellermann, T.; Kohn, N.; Gur, R.C.; Habel, U. Inhibitory control and trait aggression: Neural and behavioral insights using the emotional stop signal task. *Neuroimage* **2013**, *79*, 264–274. [CrossRef]
31. Schel, M.A.; Crone, E.A. Development of response inhibition in the context of relevant versus irrelevant emotions. *Front. Psychol.* **2013**, *4*, 383. [CrossRef]

32. Verbruggen, F.; De Houwer, J. Do emotional stimuli interfere with response inhibition? Evidence from the stop signal paradigm. *Cogn. Emot.* **2007**, *21*, 391–403. [CrossRef]
33. Lindström, B.R.; Bohlin, G. Threat-relevance impairs executive functions: Negative impact on working memory and response inhibition. *Emotion* **2012**, *12*, 384. [CrossRef]
34. Kalanthroff, E.; Cohen, N.; Henik, A. Stop feeling: Inhibition of emotional interference following stop-signal trials. *Front. Hum. Neurosci.* **2013**, *7*, 78. [CrossRef]
35. Rebetez, M.M.L.; Rochat, L.; Billieux, J.; Gay, P.; Van der Linden, M. Do emotional stimuli interfere with two distinct components of inhibition? *Cogn. Emot.* **2015**, *29*, 559–567. [CrossRef]
36. Patterson, T.K.; Lenartowicz, A.; Berkman, E.T.; Ji, D.; Poldrack, R.A.; Knowlton, B.J. Putting the brakes on the brakes: Negative emotion disrupts cognitive control network functioning and alters subsequent stopping ability. *Exp. Brain Res.* **2016**, *234*, 3107–3118. [CrossRef]
37. Huster, R.J.; Enriquez-Geppert, S.; Lavallee, C.F.; Falkenstein, M.; Herrmann, C.S. Electroencephalography of response inhibition tasks: Functional networks and cognitive contributions. *Int. J. Psychophysiol.* **2013**, *87*, 217–233. [CrossRef]
38. Knyazev, G.; Slobodskoj-Plusnin, J.Y.; Bocharov, A. Event-related delta and theta synchronization during explicit and implicit emotion processing. *Neuroscience* **2009**, *164*, 1588–1600. [CrossRef]
39. Swann, N.; Tandon, N.; Canolty, R.; Ellmore, T.M.; McEvoy, L.K.; Dreyer, S.; DiSano, M.; Aron, A.R. Intracranial EEG reveals a time-and frequency-specific role for the right inferior frontal gyrus and primary motor cortex in stopping initiated responses. *J. Neurosci.* **2009**, *29*, 12675–12685. [CrossRef]
40. Schaum, M.; Pinzuti, E.; Sebastian, A.; Lieb, K.; Fries, P.; Mobascher, A.; Jung, P.; Wibral, M.; Tüscher, O. Right inferior frontal gyrus implements motor inhibitory control via beta-band oscillations in humans. *eLife* **2021**, *10*, e61679. [CrossRef]
41. Vandierendonck, A. On the utility of integrated speed-accuracy measures when speed-accuracy trade-off is present. *J. Cogn.* **2021**, *4*, 22. [CrossRef]
42. Herz, D.M.; Tan, H.; Brittain, J.-S.; Fischer, P.; Cheeran, B.; Green, A.L.; FitzGerald, J.; Aziz, T.Z.; Ashkan, K.; Little, S. Distinct mechanisms mediate speed-accuracy adjustments in cortico-subthalamic networks. *eLife* **2017**, *6*, e21481. [CrossRef]
43. Herz, D.M.; Zavala, B.A.; Bogacz, R.; Brown, P. Neural correlates of decision thresholds in the human subthalamic nucleus. *Curr. Biol.* **2016**, *26*, 916–920. [CrossRef]
44. Cavanagh, J.F.; Zambrano-Vazquez, L.; Allen, J.J. Theta lingua franca: A common mid-frontal substrate for action monitoring processes. *Psychophysiology* **2012**, *49*, 220–238. [CrossRef]
45. Cavanagh, J.F.; Wiecki, T.V.; Cohen, M.X.; Figueroa, C.M.; Samanta, J.; Sherman, S.J.; Frank, M.J. Subthalamic nucleus stimulation reverses mediofrontal influence over decision threshold. *Nat. Neurosci.* **2011**, *14*, 1462–1467. [CrossRef]
46. Frank, M.J.; Gagne, C.; Nyhus, E.; Masters, S.; Wiecki, T.V.; Cavanagh, J.F.; Badre, D. fMRI and EEG predictors of dynamic decision parameters during human reinforcement learning. *J. Neurosci.* **2015**, *35*, 485–494. [CrossRef]
47. Aron, A.R.; Behrens, T.E.; Smith, S.; Frank, M.J.; Poldrack, R.A. Triangulating a cognitive control network using diffusion-weighted magnetic resonance imaging (MRI) and functional MRI. *J. Neurosci.* **2007**, *27*, 3743–3752. [CrossRef]
48. Forstmann, B.U.; Anwander, A.; Schäfer, A.; Neumann, J.; Brown, S.; Wagenmakers, E.-J.; Bogacz, R.; Turner, R. Cortico-striatal connections predict control over speed and accuracy in perceptual decision making. *Proc. Natl. Acad. Sci. USA* **2010**, *107*, 15916–15920. [CrossRef]
49. Lambert, C.; Zrinzo, L.; Nagy, Z.; Lutti, A.; Hariz, M.; Foltynie, T.; Draganski, B.; Ashburner, J.; Frackowiak, R. Confirmation of functional zones within the human subthalamic nucleus: Patterns of connectivity and sub-parcellation using diffusion weighted imaging. *Neuroimage* **2012**, *60*, 83–94. [CrossRef]
50. Bogacz, R.; Wagenmakers, E.-J.; Forstmann, B.U.; Nieuwenhuis, S. The neural basis of the speed–accuracy tradeoff. *Trends Neurosci.* **2010**, *33*, 10–16. [CrossRef]
51. Heathcote, A.; Lin, Y.-S.; Reynolds, A.; Strickland, L.; Gretton, M.; Matzke, D. Dynamic models of choice. *Behav. Res. Methods* **2019**, *51*, 961–985. [CrossRef] [PubMed]
52. Weigard, A.; Sripada, C. Task-General Efficiency of Evidence Accumulation as a Computationally Defined Neurocognitive Trait: Implications for Clinical Neuroscience. *Biol. Psychiatry Glob. Open Sci.* **2021**, *1*, 5–15. [CrossRef] [PubMed]
53. Battaglia, S.; Serio, G.; Scarpazza, C.; D'Ausilio, A.; Borgomaneri, S. Frozen in (e) motion: How reactive motor inhibition is influenced by the emotional content of stimuli in healthy and psychiatric populations. *Behav. Res. Ther.* **2021**, *146*, 103963. [CrossRef]
54. Bekker, E.M.; Kenemans, J.L.; Hoeksma, M.R.; Talsma, D.; Verbaten, M.N. The pure electrophysiology of stopping. *Int. J. Psychophysiol.* **2005**, *55*, 191–198. [CrossRef]
55. Kok, A.; Ramautar, J.R.; De Ruiter, M.B.; Band, G.P.; Ridderinkhof, K.R. ERP components associated with successful and unsuccessful stopping in a stop-signal task. *Psychophysiology* **2004**, *41*, 9–20. [CrossRef]
56. Boehler, C.N.; Münte, T.F.; Krebs, R.M.; Heinze, H.-J.; Schoenfeld, M.A.; Hopf, J.-M. Sensory MEG responses predict successful and failed inhibition in a stop-signal task. *Cereb. Cortex* **2009**, *19*, 134–145. [CrossRef]
57. Wessel, J.R. Prepotent motor activity and inhibitory control demands in different variants of the go/no-go paradigm. *Psychophysiology* **2018**, *55*, e12871. [CrossRef]
58. Wessel, J.R.; Aron, A.R. It's not too late: The onset of the frontocentral P 3 indexes successful response inhibition in the stop-signal paradigm. *Psychophysiology* **2015**, *52*, 472–480. [CrossRef]

59. Steinemann, N.A.; O'Connell, R.G.; Kelly, S.P. Decisions are expedited through multiple neural adjustments spanning the sensorimotor hierarchy. *Nat. Commun.* **2018**, *9*, 3627. [CrossRef]
60. Groen, I.I.; Jahfari, S.; Seijdel, N.; Ghebreab, S.; Lamme, V.A.; Scholte, H.S. Scene complexity modulates degree of feedback activity during object detection in natural scenes. *PLoS Comput. Biol.* **2018**, *14*, e1006690. [CrossRef]
61. Tu, Y.-Z.; Lin, D.-W.; Suzuki, A.; Goh, J.O.S. East Asian young and older adult perceptions of emotional faces from an age-and sex-fair east Asian facial expression database. *Front. Psychol.* **2018**, *9*, 2358. [CrossRef] [PubMed]
62. Delorme, A.; Makeig, S. EEGLAB: An open source toolbox for analysis of single-trial EEG dynamics including independent component analysis. *J. Neurosci. Methods* **2004**, *134*, 9–21. [CrossRef] [PubMed]
63. Grandchamp, R.; Delorme, A. Single-trial normalization for event-related spectral decomposition reduces sensitivity to noisy trials. *Front. Psychol.* **2011**, *2*, 236. [CrossRef] [PubMed]
64. Senderecka, M. Threatening visual stimuli influence response inhibition and error monitoring: An event-related potential study. *Biol. Psychol.* **2016**, *113*, 24–36. [CrossRef] [PubMed]
65. Ratcliff, R.; McKoon, G. The diffusion decision model: Theory and data for two-choice decision tasks. *Neural Comput.* **2008**, *20*, 873–922. [CrossRef]
66. Wiecki, T.V.; Sofer, I.; Frank, M.J. HDDM: Hierarchical Bayesian estimation of the drift-diffusion model in Python. *Front. Neuroinformatics* **2013**, *7*, 14. [CrossRef]
67. Williams, S.E.; Lenze, E.J.; Waring, J.D. Positive information facilitates response inhibition in older adults only when emotion is task-relevant. *Cogn. Emot.* **2020**, *34*, 1632–1645. [CrossRef]
68. Carretié, L. Exogenous (automatic) attention to emotional stimuli: A review. *Cogn. Affect. Behav. Neurosci.* **2014**, *14*, 1228–1258. [CrossRef]
69. Cohen, M.X. A neural microcircuit for cognitive conflict detection and signaling. *Trends Neurosci.* **2014**, *37*, 480–490. [CrossRef]
70. Matzke, D.; Logan, G.D.; Heathcote, A. A cautionary note on evidence-accumulation models of response inhibition in the stop-signal paradigm. *Comput. Brain Behav.* **2020**, *3*, 269–288. [CrossRef]
71. Yau, Y.; Hinault, T.; Taylor, M.; Cisek, P.; Fellows, L.K.; Dagher, A. Evidence and urgency related EEG signals during dynamic decision-making in humans. *J. Neurosci.* **2021**, *41*, 5711–5722. [CrossRef] [PubMed]